Proceeding sof SPIE on Signal processing, Sensor Fusion, and target Recognition XI (Vol. 4729), Ilvan Kadar, Editor, Orlando FL, 1-3 April 2002.

# Cross-Sensor Image Fusion and Spectral Anomaly Detection

Mark J. Carlotto (mark.carlotto@veridian.com)
Veridian Systems Division
1400 Key Blvd., Suite 100
Arlington VA 22209

**Abstract**

A nonlinear mean square estimation algorithm for cross-sensor image fusion and spectral anomaly detection is described. The algorithm can be used to enhance a low resolution image with a higher resolution coregistered multispectral image, and to detect anomalies between spectral bands (features in one spectral band that do not occur in other bands). Experimental results for Landsat data are presented illustrating the spatial enhancement of thermal imagery, the detection of thermal anomalies (heat sources), and the detection of smoke plumes.

## Introduction

A variety of methods have been developed for fusing multisensor imagery for band sharpening, feature classification, and object/change detection. Examples include principal components (Li, Zhou, and Li, 1999), wavelet transforms (Gomez, Jazaeri, and Kafatos, 2001; Lemeshewsky, 1999), pseudoinverse estimation and fuzzy reasoning (Patterson, Bullock and Wada 1992), and linear prediction (Tom, Carlotto, and Scholten 1985) for band sharpening; spectral mixing models (Gross and Schott, 1996) and neural networks (Shaikh, Tian, Azimi-Sadjadi, Eis, and Vonder Haar, 1996) for classification; signal subspace processing (Soumekh 1998), neural networks (Brown, Derouin, Beck, and Archer, 1992), and nonlinear transforms (Carlotto 2000) for multisensor/multispectral object/change detection.

This paper describes the application of a nonlinear mean-square estimation technique originally developed for multispectral haze reduction (Carlotto 1999) to the detection of manmade objects and activities using a cross-spectral anomaly detection approach. The anomaly detector operates under the assumption that over natural backgrounds there is a high degree of correlation between spectral bands. Manmade activities, on the other hand, alter selected portions of the spectrum and thus introduce spectral anomalies at certain wavelengths. We use a nonlinear mean-square estimator to segment one set of spectral bands into different background types, and predict the average response over each background type in another set of bands. Spectral anomalies (pixels whose value differs from other pixels of the same background type) are detected based on the difference between their actual and predicted values.

## Method

Our approach is based on using a nonlinear mean-square estimator to estimate an output image $y$ from a set of coregistered input images $\mathbf{x}$. The estimator is a nonlinear mapping $\tilde{y} = f[\mathbf{x}]$ between the two image spaces. Papoulis (1965) shows that the optimal estimator is the conditional expected value $f = E[y|\mathbf{x}]$. Note that because $f$ depends on $y$, the estimator is not predictive; i.e., it assumes that the quantity being estimated is actually known.

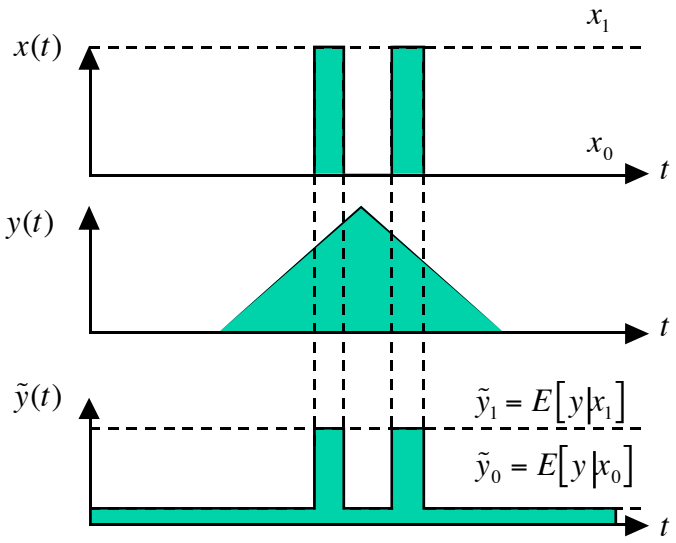


*Fig. 1 Spatial enhancement example*

Consider two signals, $x(t)$ and $y(t)$. Assume the first is from a high resolution sensor that is able to resolve two closely-spaced objects, while the second is from a lower resolution sensor that is unable to resolve the objects (Fig. 1). By graphically constructing the conditional expected value, it is evident that the two objects can be resolved in the estimate $\tilde{y}(t)$.

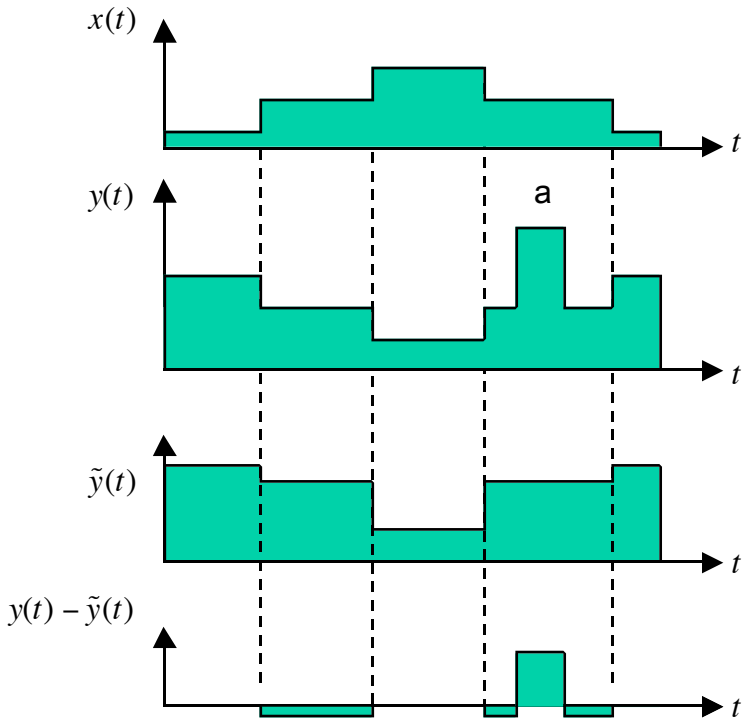


*Fig.2 Anomaly detection example*

In Fig. 1 the two signals were at different resolutions but correlated. Fig. 2 depicts two signals that are highly correlated everywhere except over a short interval containing an anomalous pulse (a). Because the pulse is not present in the first signal, it is missing in the estimate $\tilde{y}(t)$ and thus shows up as an anomaly in the difference $y(t) - \tilde{y}(t)$.

Fig. 3 shows a cross-spectral anomaly detector that uses one set of predictor bands to estimate another set of target bands (possibly at a different spatial resolution). The nonlinear estimate is a lookup table that is applied to the predictor bands to form a set of estimated target bands. Anomalous pixels are those whose difference exceeds a predetermined threshold.

## Thermal Band Sharpening

Fig. 3a shows part of a Landsat TM thermal band image over Boston MA. The resolution of this image is 120 meters/pixel. Fig. 3b is the sharpened thermal band image produced by the nonlinear estimator operating on three visible/reflective IR band images (bands 2, 4, and 7) at 30 meters/pixel. Notice the patterns of runways and streets in the sharpened image. Also notice the diagonal striping pattern caused by the thermal band detector's array fixed pattern noise is removed in the sharpened image. The black region near bottom of the image is a cloud.

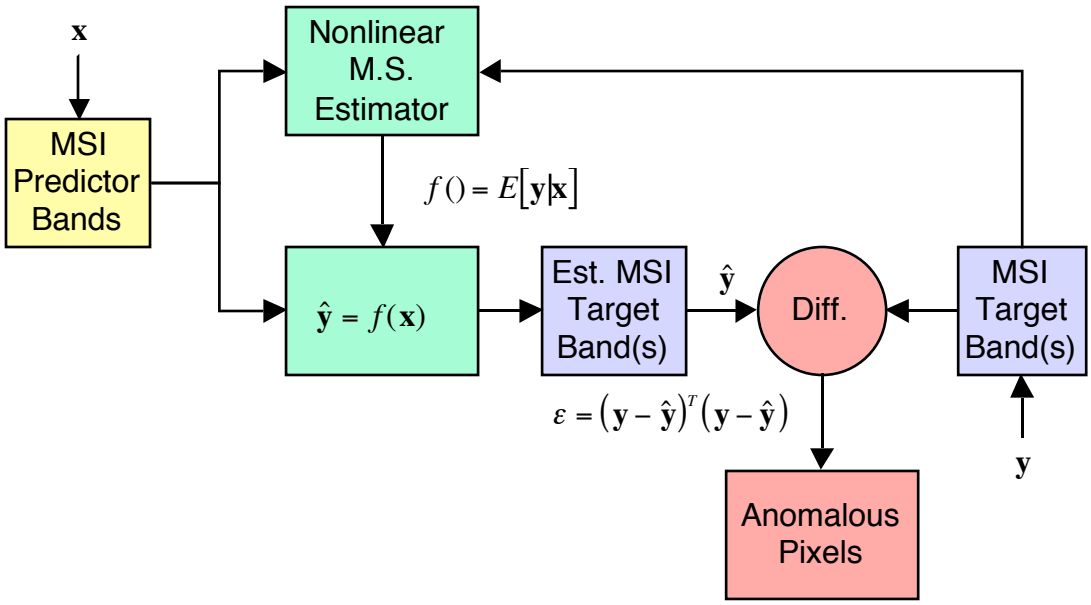


*Fig. 3 Cross-spectral anomaly detection process*

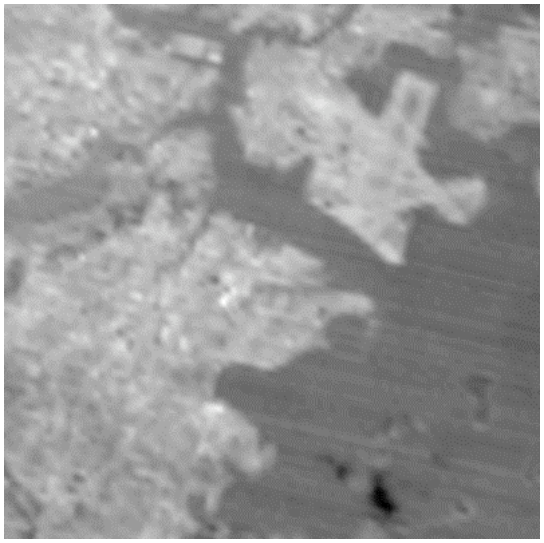

*a) Landsat TM thermal band image over Boston MA.*

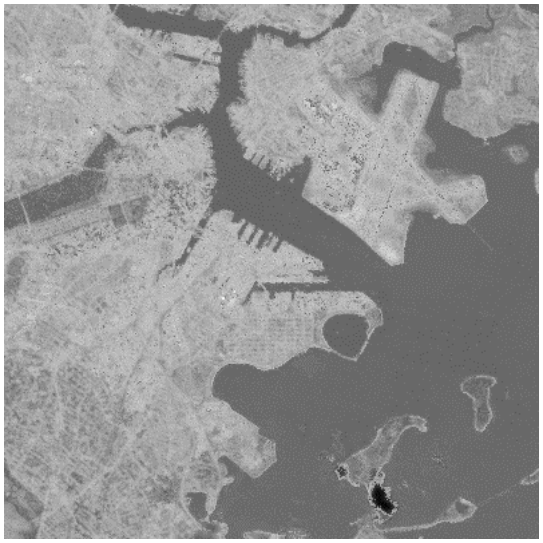

*b) Thermal band sharpened using TM bands 2, 4, and 7.*

*c) Difference between actual and predicted thermal band images*

*Fig. 3 Thermal band sharpening example*

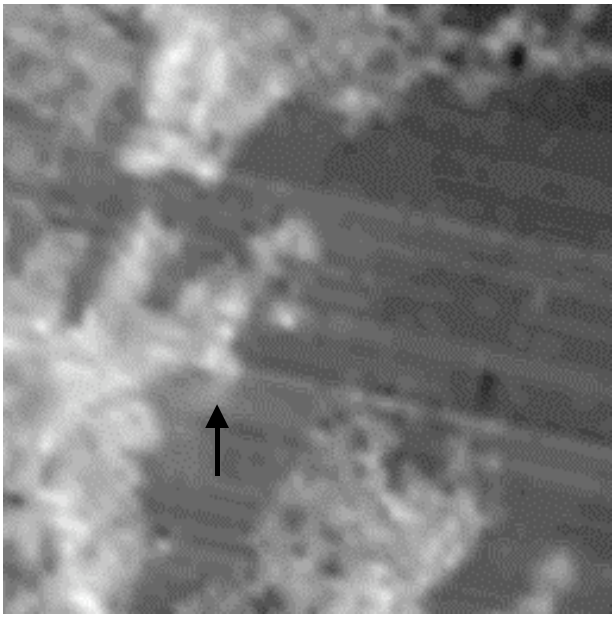

*a) TM thermal band image*

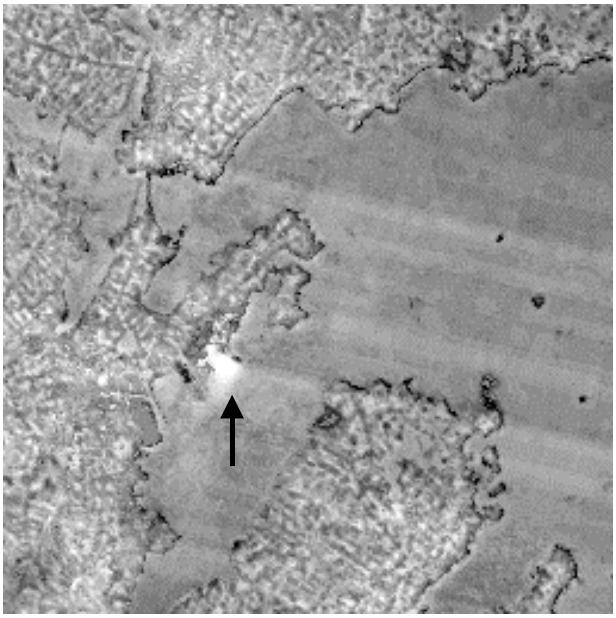

*b) Thermal band estimated from TM bands 2,4, and 7.*

*Fig. 4 Thermal anomaly detection example*

## Thermal Anomaly Detection

One expects that similar materials under similar conditions will be at similar temperatures. As shown in Fig. 3c, edge effects aside, differences exist between the higher resolution thermal band estimate and the original thermal band image. In many cases these differences are caused by manmade activities. Farther up the coast, in Salem MA, is a coal burning power plant at Salem Willows (Fig. 4). In the original thermal band image (a) the thermal discharge from the powerplant into the harbor is not evident. Because the temperature of the water is much less than the land, the heat of the adjacent urban areas of Beverly and Salem dominate. But because the thermal discharge is not evident in Landsat's visible and near infrared bands, a difference exists between the actual and predicted thermal band values in the vicinity of the powerplant (b).

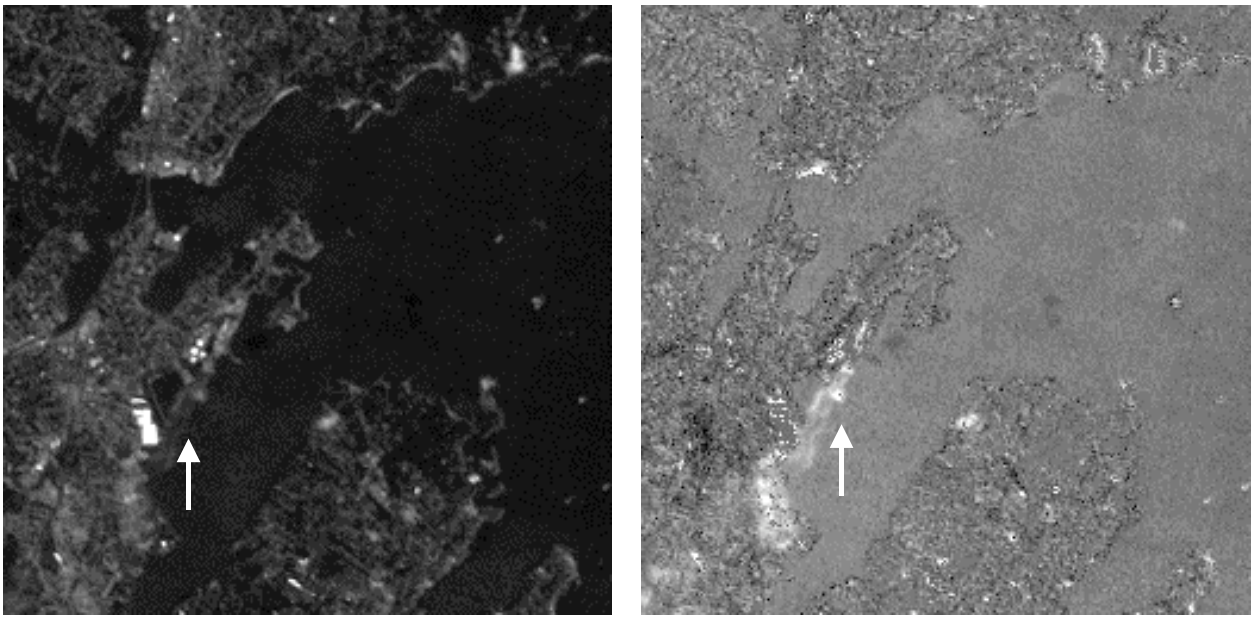

*a) TM band 1 (blue)* *b) Band 1 estimated from bands 4, 5, and 7.*

*Fig. 5 Visible-reflective IR anomaly detection example*

## Visible-Reflective IR Anomaly Detection

A similar opportunity exists between the visible and reflective IR bands for detecting the smoke plume from the powerplant. Previously it has been shown that it is possible to use the nonlinear mean-square estimator to remove wavelength-selective scattering phenomena from the visible bands by using information from the reflective IR bands (Carlotto 1999). Here we use the difference between the original and the haze-free estimate to detect the haze and smoke (Fig. 5).

Again as in Fig. 4 the feature of interest, in this case the smoke, is not evident in the origin image (a) but is significantly enhanced in the difference image (b).

## Discussion

In order to detect manmade objects/activities using a single sensor the activity must be both visible to the sensor and distinct enough from the background to be detectable. This is particularly difficult in heavily vegetated areas where the activity may be concealed under canopy, or in urban areas where it can blend into the background. In thermal imagery, subtle temperature differences within a material type (e.g., trees) may not be noticeable in an image when large differences between materials (trees and open areas) are present nearby. Because materials in the scene are at different temperatures, one must know the material (background type) in order to assess its thermal state. The nonlinear estimator effectively segments an image into $K$ different background types (spectral vectors). The conditional expectation over the k-th background $E[y|\mathbf{x}_k]$ provides a normalcy model for detecting anomalies within that background type. The model assumes that pixels with a similar (but in general, unknown) value in one set of bands will have a similar (but also unknown) value in a second set of bands. The nonlinear estimator determines the expected value in the second set of bands. In this way subtle differences within background types can be detected.

### *References*

Gomez, Richard B.; Jazaeri, Amin; Kafatos, Menas, Wavelet-based hyperspectral and multispectral image fusion, Proc. SPIE Vol. 4383, p. 36-42, *Geo-Spatial Image and Data Exploitation II*, William E. Roper; Ed., 2001.

Carlotto, M.J., "Nonlinear Background Estimation and Change Detection for Wide Area Search," *Optical Engineering*, Vol. 39, No. 5, pp 1223-1229, May 2000.

Carlotto, M.J., "Reducing the Effects of Space-Varying Wavelength-Dependent Scattering in Multispectral Imagery," *International Journal of Remote Sensing*, Vol. 20, No. 17, pp 3333-3344, 1999.

Li, Jun; Zhou, Yueqin; Li, Deren, PCA and wavelet transform for fusing panchromatic and multispectral images, Proc. SPIE Vol. 3719, p. 369-377, *Sensor Fusion: Architectures, Algorithms, and Applications III*, Belur V. Dasarathy; Ed., 1999.

Lemeshewsky, George P., Multispectral multisensor image fusion using wavelet transforms, Proc. SPIE Vol. 3716, p. 214-222, *Visual Information Processing VIII*, Stephen K. Park; Richard D. Juday; Eds., 1999.

Soumekh, Mehrdad, Moving-target detection and automatic target recognition via signal subspace fusion of images, Proc. SPIE Vol. 3370, p. 120-131, *Algorithms for Synthetic Aperture Radar Imagery V*, Edmund G. Zelnio; Ed., 1998.

Agassi, Eyal; Ben-Yosef, Nissim, Relation between thermal infrared and visible/near-infrared images of natural scenes: an overview, Proc. SPIE Vol. 3110, p. 127-135, *10th Meeting on Optical Engineering in Israel*, Itzhak Shladov; Stanley R. Rotman; Eds.,1997.

Gross, Harry N.; Schott, John R., Evaluating an image-fusion algorithm with synthetic image generation tools, Proc. SPIE Vol. 2758, p. 136-147, *Algorithms for Multispectral and Hyperspectral Imagery II*, A. Evan Iverson; Ed., 1996.

Shaikh, Mukhtiar A.; Tian, Bin; Azimi-Sadjadi, Mahmood R.; Eis, Kenneth E.; Vonder Haar, Thomas H., Automatic neural network-based cloud detection/classification scheme using multispectral and textural features, Proc. SPIE Vol. 2758, p. 51-61, *Algorithms for Multispectral and Hyperspectral Imagery II*, A. Evan Iverson; Ed., 1996.

Brown, Joe R.; Derouin, Edward E.; Beck, Hal E.; Archer, Susan J., Hyperspectral data fusion for target detection using neural networks Proc. SPIE Vol. 1623, p. 202-202, *The 20th AIPR Workshop: Computer Vision Applications--Meeting the Challenges*, Joan B. Lurie; Ed.,1992.

Patterson, Tim J.; Bullock, Michael E.; Wada, Alan D., Multispectral band sharpening using pseudoinverse estimation and fuzzy reasoning, Proc. SPIE Vol. 1693, p. 170-181, *Surveillance Technologies II*, Sankaran Gowrinathan; James F. Shanley; Eds., 1992.

Tom, V.T.; Carlotto, M.J.; and Scholten, D,J.,"Spatial sharpening of Thematic Mapper data using a multiband approach," *Optical Engineering*, Vol. 24, No. 6, 1985.

Papoulis, A., *Probability, Random Variables, and Stochastic Processes*, McGraw Hill, 1965.